

# Geophysical Research Letters<sup>®</sup>



## RESEARCH LETTER

10.1029/2021GL097386

### Key Points:

- We present an innovative method to quantify the processes that lead to a modeled increase in stratospheric water vapor from increased CO<sub>2</sub>
- As well as changes in large-scale temperatures and transport, we find convective injection of ice contributes to stratospheric moistening
- The frequency of convective injection increases as CO<sub>2</sub> increases, but its relative contribution to stratospheric water vapor does not

### Supporting Information:

Supporting Information may be found in the online version of this article.

### Correspondence to:

J. W. Smith,  
[jws52@cam.ac.uk](mailto:jws52@cam.ac.uk)

### Citation:

Smith, J. W., Bushell, A. C., Butchart, N., Haynes, P. H., & Maycock, A. C. (2022). The effect of convective injection of ice on stratospheric water vapor in a changing climate. *Geophysical Research Letters*, 49, e2021GL097386. <https://doi.org/10.1029/2021GL097386>

Received 13 DEC 2021  
Accepted 28 MAR 2022

## The Effect of Convective Injection of Ice on Stratospheric Water Vapor in a Changing Climate

Jacob W. Smith<sup>1</sup> , Andrew C. Bushell<sup>2</sup> , Neal Butchart<sup>2</sup> , Peter H. Haynes<sup>3</sup> , and Amanda C. Maycock<sup>4</sup> 

<sup>1</sup>Department of Plant Sciences, University of Cambridge, Cambridge, UK, <sup>2</sup>Met Office Hadley Centre, Exeter, UK,

<sup>3</sup>Department of Applied Mathematics and Theoretical Physics, University of Cambridge, Cambridge, UK, <sup>4</sup>School of Earth and Environment, University of Leeds, Leeds, UK

**Abstract** Stratospheric water vapor affects the Earth's radiative balance and stratospheric chemistry, yet its future changes are uncertain and not fully understood. The influence of deep convection on stratospheric water vapor remains subject to debate. This letter presents a detailed process-based model study of the impact of convective ice sublimation on stratospheric water vapor in response to CO<sub>2</sub> forced climate change. The influence of convective injection is found to be limited by the vertical profile of temperature and saturation vapor pressure in the tropical tropopause layer, not by the frequency of occurrence. Lagrangian trajectory analysis shows the relative contributions to stratospheric water vapor from sublimation and large-scale transport are approximately unchanged when CO<sub>2</sub> is increased. The results indicate the role of convective ice injection for stratospheric water vapor in a warmer climate remains constrained by large-scale temperatures.

**Plain Language Summary** Trends in stratospheric water vapor impact on both ozone depletion and the climate. Water vapor enters the stratosphere in the tropics and is tightly constrained by the cold temperatures around the tropopause (around 15–17 km altitude). For the present day climate the contribution from the direct injection of ice into the stratosphere by deep convection is thought to be relatively small, but it has been suggested these may increase in a warmer climate. If convection becomes more frequent and stronger under greenhouse gas induced climate change, the response of stratospheric water vapor might be different from that implied simply by changes to tropical tropopause temperatures. This study examines the roles of convection and large-scale temperatures and transport in determining the water budget in the tropical tropopause region in a climate model. In response to increased atmospheric carbon dioxide the model simulates increased stratospheric water vapor with a substantial contribution coming from more convective injection. However, the relative contribution of convective injection to stratospheric water vapor remains roughly constant as carbon dioxide increases. Therefore, irrespective of whether convection becomes stronger or more frequent, the impact of convective injection of water is found to be constrained by large-scale temperatures.

## 1. Introduction

Changes in stratospheric water vapor can have a significant effect on Earth's energy balance and global surface temperature change (e.g., Forster & Shine, 2002; Manabe & Wetherald, 1967; Solomon et al., 2010). Stratospheric water vapor changes also affect stratospheric chemistry, through effects on HO<sub>x</sub> radicals (Stenke & Grewe, 2005) and polar stratospheric clouds (Kirk-Davidoff et al., 1999), as well as stratospheric temperature trends (Forster & Shine, 2002; Maycock et al., 2014; Oinas et al., 2001) and global circulation (Maycock et al., 2013). Current climate models in phase six of the Coupled Model Intercomparison Project (CMIP6) show a large spread in stratospheric water vapor concentrations in the present day and in future projections (Keeble et al., 2021). This in turn implies large uncertainty in the climate feedback induced by future changes in stratospheric water vapor (Banerjee et al., 2019). It is therefore important to understand the processes that control stratospheric water vapor concentrations and their representation in general circulation models (GCMs) to develop strategies to reduce the uncertainty in projections.

Water vapor concentrations in the stratospheric overworld (above ~380 K potential temperature) are largely determined by freeze-drying processes in the tropical tropopause layer (TTL; Fueglistaler et al., 2009) and moistening due to methane oxidation. In the lowermost extratropical stratosphere, an additional influence is mixing of air from the stratospheric overworld with moist air from the troposphere. This paper will focus on the freeze-drying

© 2022 Crown copyright. This article is published with the permission of the Controller of HMSO and the Queen's Printer for Scotland.

This is an open access article under the terms of the [Creative Commons Attribution License](https://creativecommons.org/licenses/by/4.0/), which permits use, distribution and reproduction in any medium, provided the original work is properly cited.

in the TTL. However, it should be kept in mind that water vapor changes in the lowermost stratosphere are also important for the global radiative balance (Banerjee et al., 2019; Maycock et al., 2011).

A simple advection-condensation calculation, in which water vapor concentrations of air parcels are set by the minimum saturation mixing ratio encountered in transit through the TTL, is adequate to capture water vapor temporal variability, but is biased dry compared to observations (Liu et al., 2010). This bias is due to missing processes such as convective transport and other small-scale processes, as well as microphysical details of particle formation and sedimentation. The influence of deep convection on stratospheric water vapor has been long debated. Though there has been occasional observational evidence for convective dehydration (e.g., Khaykin et al., 2022), convective penetration and accompanying hydration by transport of ice and water vapor above the local cold point have been frequently observed (e.g., Khaykin et al., 2009; Lee et al., 2019) and modeled (e.g., Dauhut et al., 2018). An important role for convective injection of ice in determining lower stratospheric humidity has been observed outside of the tropics (e.g., Schwartz et al., 2013; Werner et al., 2020). Nevertheless, recent large-scale estimates have suggested that the overall effect of convective hydration on global-scale stratospheric water vapor concentrations is modest (e.g., Schoeberl et al., 2018; Wright et al., 2011).

As the surface and troposphere warm due to anthropogenic climate change, deep convective systems may be expected to become more energetic (e.g., Romps, 2011). This raises the possibility that convective hydration may become more important for stratospheric water vapor in the future. Dessler et al. (2016) (hereafter D2016) examined two chemistry-climate models in which stratospheric water vapor was simulated to increase over the 2000–2100 period and determined from trajectory-based calculations that large-scale TTL temperatures changes could only account for 50%–80% of the total stratospheric water vapor change. By incorporating a simple scheme for hydration by convective injection of ice into an advection-condensation calculation, D2016 improved the match between predicted and actual water vapor anomalies. While the D2016 conclusion ‘...solid evidence exists that trends in convectively lofted ice evaporation drive a significant part of the 21st century trend in  $\text{H}_2\text{O}_{\text{entry}}$ ’ is interesting, relatively few details of the model simulations are given and a number of questions remain. Moreover, few studies have tested this conclusion in other models or compared the simplified trajectory-based calculations with a full TTL moisture budget analysis in GCMs.

This paper sheds further light on the role of convective injection for stratospheric water vapor in a GCM, both for the current climate and with increased greenhouse gas amounts. Section 2 describes the model and methods. Section 3 presents an innovative method to quantify the processes that lead to a modeled increase in stratospheric water vapor from increased  $\text{CO}_2$  concentrations. Section 4 presents trajectory-based calculations to determine which processes control the response of stratospheric water vapor to a doubling and quadrupling of  $\text{CO}_2$  concentrations. Conclusions are given in Section 5.

## 2. Methods

### 2.1. Global Climate Model

We use the same Global Atmosphere configuration model (GA7.0; Walters et al., 2019) as in HadGEM3-GC3.1 (Hadley Centre Global Environmental Model version 3 with Global Coupled configuration 3.1) and UKESM1 (United Kingdom Earth System Model version 1), which contributed to CMIP6 (Eyring et al., 2016). The model timestep is 20 min with a horizontal resolution of  $1.875^\circ$  longitude  $\times$   $1.25^\circ$  latitude and 85 vertical levels extending to  $\sim 85$  km. Levels in the TTL are separated by about 700 m. The model includes water in vapor phase and liquid or ice cloud condensate. In the TTL, temperatures are sufficiently low that liquid condensate is absent, therefore this phase will not be considered further.

We investigate three time-slice simulations with constant seasonally-varying boundary conditions. The control simulation (referred to as CONTROL) has fixed year 2002 boundary conditions (including sea surface temperatures [SSTs], atmospheric composition and solar insolation). The second and third simulations (referred to as  $2 \times \text{CO}_2$  and  $4 \times \text{CO}_2$ ) have, respectively, doubled and quadrupled  $\text{CO}_2$  concentrations from a 2002 reference state, and SSTs increased uniformly by 2 K and 4 K. These simulations match experiments 2, 3 and 4 of the Quasi-Biennial Oscillation initiative (Bushell et al., 2020; Butchart et al., 2018; Richter et al., 2020). Each simulation was integrated with 21 years of repeat annual cycle forcing. To allow for spin-up, the analysis in Section 4 is based on the last 10 years when the relevant variables have stabilized.

For the analysis in Section 3, increments to ice and to water vapor from all individual model parameterization schemes which contribute to the moisture budget were evaluated and stored at 6-hourly intervals. A sensitivity test using higher frequency sampling did not change monthly mean values. The water vapor and ice budgets were only assessed for the first 2 years of the decade used for analysis in each simulation, due to the large computer resource required to store all increments. The principal contributions included in the analysis for both ice and water vapor are: transport by the model velocity field (advection); transport by the convective parametrization (convection); and net conversion from the other phases taking account of sublimation and deposition (net phase change). For ice, sedimentation is also included.

As it is useful for some purposes to consider whether or not non-zero increments due to different model processes are located above or below the model tropopause, we define at each horizontal location the ‘dry-point tropopause’ as the level where the vertical minimum in saturation mixing ratio occurs.

## 2.2. Lagrangian Calculations

Following Smith et al. (2021), back trajectory calculations were performed with the Lagrangian transport model OFFLINE (Liu et al., 2010; Methven, 1997). These were based on 6-hourly three-dimensional fields output from the GCM including velocity, temperature and pressure. For each GCM simulation, back trajectories were initialized monthly at 75 hPa (~18.2 km) on a  $2^\circ \times 2^\circ$  grid between  $30^\circ\text{N}$  and  $30^\circ\text{S}$  (i.e., 5,580 trajectories for each month). The timestep for the trajectory calculation was 36 min, with velocity fields linearly interpolated between neighboring time points. Points along the trajectories were stored at 6-hr intervals, along with the model fields interpolated to these trajectory locations.

Saturation mixing ratios were calculated using local temperature and pressure following the formulation of Wagner et al. (2011). As in Liu et al. (2010) and Smith (2020) the Lagrangian Dry Point (LDP) of a trajectory is calculated as the minimum in saturation mixing ratio during its history. Water vapor concentrations entering the stratosphere for a given date ( $q_{LDP}$ ) are estimated by averaging the LDP saturation mixing ratio of any back trajectories which were initialized at that time and reached the troposphere (defined as potential temperature  $<340$  K and saturation mixing ratio  $>1,000$  ppmv) within 360 days. The  $q_{LDP}$  estimates were found to be insensitive to increased horizontal density of trajectories or to more frequent release.

In order to account for ice sublimation into subsaturated air parcels, the local *ice water content* (also simulated at 6-hr intervals across the 10 model years used for analysis) and increments for *net phase change* and *convective ice injection*, which relate to sublimation, were applied to modify the LDP calculations. For the most straightforward calculation, if an air parcel was subsaturated at any point along its trajectory and ice was present, then available ice was assumed to sublimate immediately, until the water vapor concentration reached saturation. Note that this only impacts the predicted final water vapor concentration ( $q_{LDP+ice}$ ) if ice is encountered after the LDP (i.e., the final dehydration location according to the standard calculation).

This  $q_{LDP+ice}$  calculation differs from that in D2016 because they perform the adjustment at intervals defined by their trajectory time step (20 min) rather than the 6-hourly intervals at which their model fields were also available. Both choices are only approximate as both ignore the depletion of ice concentration that accompanies the conversion from ice to water. Thus a subsaturated parcel which encountered small ice concentrations might undergo multiple adjustments to emerge with a water vapor mixing ratio that depended purely on the number of adjustments that were made. This arbitrariness in the adjustment was explored with alternative specifications to provide a range of predictions for water vapor concentration as predicted by advection-condensation plus adjustment for convective hydration. Details are given in the Supporting Information S1.

## 3. GCM Water Budget and Deep Convection

For the CONTROL simulation, the height (model level) of the dry point in the tropical mean (averaged zonally and over the  $30^\circ\text{N}$ – $30^\circ\text{S}$  belt) saturation mixing ratio is 16.7 km. At the three model levels immediately above (17.4, 18.0, and 18.8 km), the tropical mean ice budget is essentially a balance between convective injection and the subsequent sedimentation of ice (Figures 1a and 1c. Note the 18.8 km level is not shown). A small additional contribution comes from large-scale transport (advection) while in-situ phase changes have a minimal effect

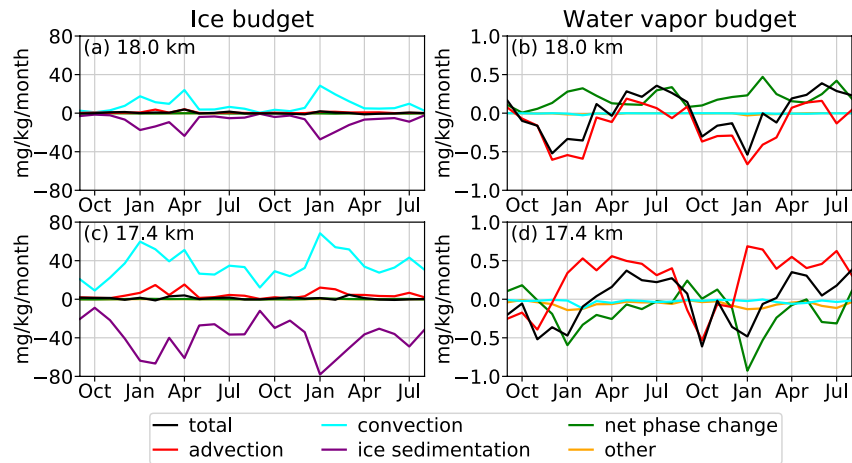


**Figure 1.** Monthly tropical (30°N–30°S) zonal mean of the general circulation models instantaneous increments for budgets of (a) ice and (b) water vapor at 18 km across 2 years of the CONTROL simulation (see text for details). Increments are scaled up to units of  $\text{mg}_{\text{H}_2\text{O}}/\text{kg}_{\text{moist-air}}/\text{month}$ . Panels (c and d) show ice and water vapor budgets at 17.4 km, the model level beneath 18 km. ‘Net phase change’ is the combination of deposition and sublimation, ‘other’ combines all other model increments.

being around 1% of the magnitude of convective injection or sedimentation. There is a decrease in magnitude of each process with height.

The contribution of phase changes is much more significant for the water vapor budget (Figures 1b and 1d—note the different scale on the y-axes from panels a and c). Net phase change increments are composed of two opposing contributions: in-situ ice formation (deposition) which decreases water vapor concentrations, and sublimation which increases it. At 17.4 km, the net phase change increment is negative in most months, indicating the dominance of deposition over sublimation, and vice-versa at 18.0 km. The transition from a dominance of deposition at 17.4 km and the levels immediately below, to a dominance of sublimation at 18 km is as expected from the increase of temperature, and hence in saturation mixing ratio, with height.

Because convective injection is the largest supplier of ice at altitudes of 17.4 km (Figures 1c), 18 km (Figure 1a), and 18.8 km (not shown), we infer that most sublimation originates from convective ice injection and can therefore be interpreted as convective hydration. There is a small contribution of around 15% to the ice budget from advection, which provides ice that is likely to have arrived either convectively or from in-situ formation (deposition). The convective hydration at 18 km is balanced by large-scale transport (advection) which together account almost entirely for the seasonal variations in water vapor (Figure 1b). At 17.4 km (Figure 1d) both the dehydration from deposition and transport contribute to the seasonal variation in water vapor (Smith et al., 2021).

To account for variability in tropical tropopause altitude, we explicitly test for convective hydration above the tropical tropopause by analyzing individual grid points located between 30°N and 30°S in the 2 years of 6-hourly GCM data available (Section 2.1). The fractional vertical distribution of the data points where convective ice injection or net sublimation (positive water vapor increment from net phase change) occurs above the instantaneous dry point tropopause are shown in Figures 2a and 2b, respectively, on model levels. Similarly, Figures 2c and 2d show the fraction of the same events in tropopause-relative height coordinates. The CONTROL,  $2 \times \text{CO}_2$ , and  $4 \times \text{CO}_2$  simulations are shown as blue, orange, and green bars, respectively. Figure 2e compares the number of net sublimation and convective ice injection events with mean increment per event for the three forcing simulations.

A role for convective hydration above the tropical tropopause is supported by the rather good agreement between the vertical distributions of net sublimation events and the convective transport of ice (‘convection events’) above the dry point, both in absolute altitude and in altitude relative to the dry point (blue bars in Figures 2a–2d). This good agreement is also seen in the  $2 \times \text{CO}_2$  and  $4 \times \text{CO}_2$  simulations (orange and green bars, respectively), though the overall distributions are shifted upwards due to the upward displacement of the dry points. In both the  $2 \times \text{CO}_2$  and  $4 \times \text{CO}_2$  simulations the stratosphere cools above about 19 km while the lapse rate in the tropical

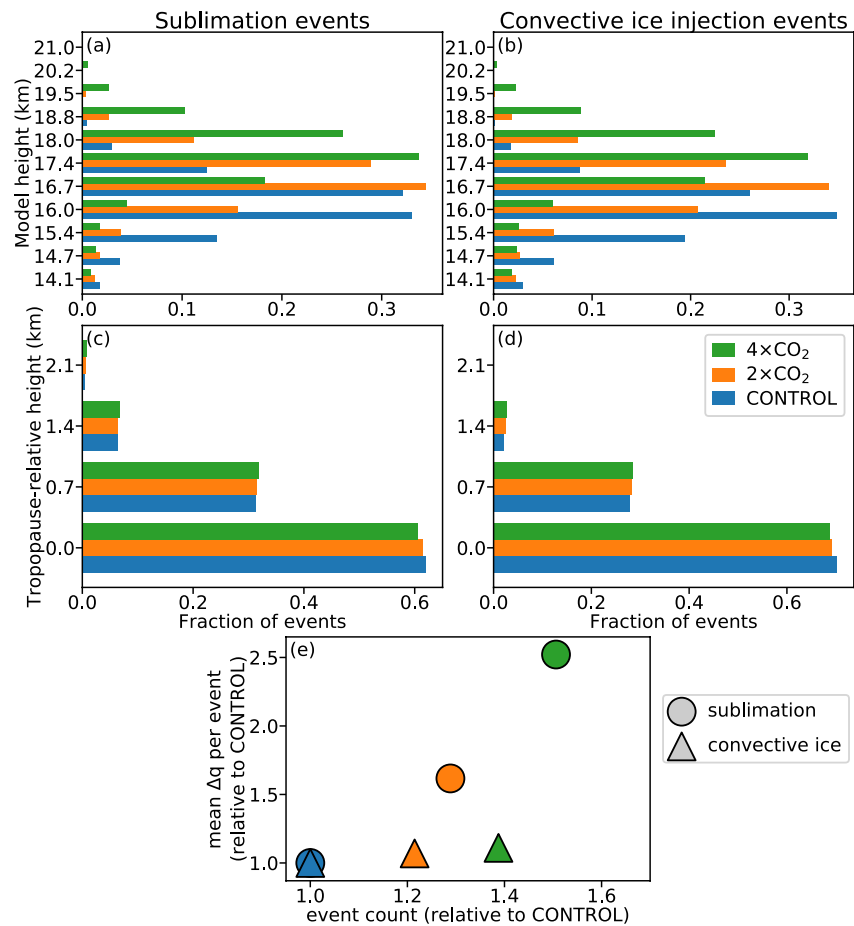


**Figure 2.** Analysis of grid points exhibiting (a, c and e) net sublimation and (b, d and e) convective ice injection above the dry-point tropopause within 30°N–30°S and in a 2 year period of 6-hourly instantaneous model increments for each climate forcing simulation. The figure shows the vertical distribution of such events as a function of (a and b) model height and (c and d) height relative to the dry-point tropopause. (e) shows, for each scenario, the number of events and average increment per event relative to CONTROL for which net sublimation event count is  $1.3 \times 10^6$  and mean increment is  $0.057 \text{ mg/kg/20 min}$ ; convective injection event count is  $1.5 \times 10^5$  and mean increment is  $29.8 \text{ mg/kg/20 min}$ .

troposphere decreases due to the temperatures increasing more in the upper troposphere than lower stratosphere, consistent with other studies (Kim et al., 2013; Lin et al., 2017). Consequently in the  $2 \times \text{CO}_2$  simulation the dry points move up one model level ( $\sim 0.7 \text{ km}$ ), and the dry point temperature and saturation mixing ratio increase by about 2.5 K and 5 ppmv, from 195 K and  $\sim 8 \text{ ppmv}$  in the CONTROL simulation, respectively. Corresponding changes in the  $4 \times \text{CO}_2$  simulation are roughly double these. When this upward shift of the dry points is taken into account, the vertical distribution of sublimation and convection events are then remarkably similar across all three simulations (Figures 2c and 2d).

In contrast, there are differences between the simulations in the number of events and in the amounts of ice injected and sublimated as the amount of  $\text{CO}_2$  is increased (Figure 2e). In the  $4 \times \text{CO}_2$  simulation compared to CONTROL, the event count for convective ice injection increases by 39% (Figure 2e, green triangle), indicating more frequent convective injection. The mean increment per event for convective ice injection also increases by 11%. However, the response of sublimation is stronger: the event count increases by 51% and the mean increment per event increases by 52% (green circle in Figure 2e). Sublimation responds more strongly than convective ice injection because the amount of ice that is sublimated is enhanced by a warmer tropical tropopause, and hence higher saturation mixing ratios, as  $\text{CO}_2$  concentration increases.

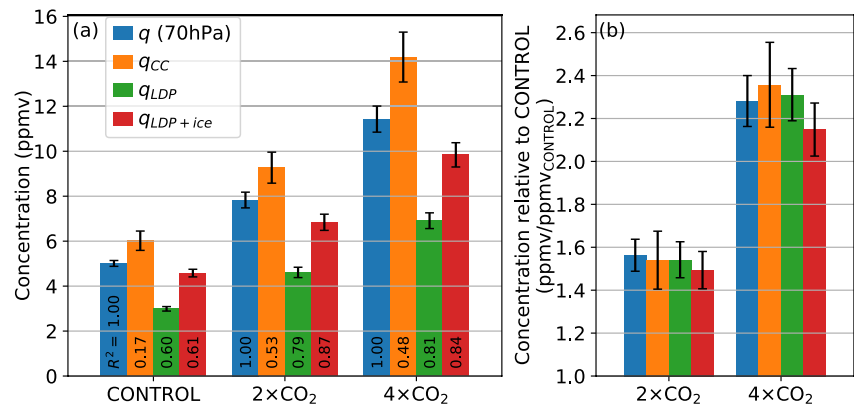


**Figure 3.** (a) 10-year tropical ( $30^\circ\text{N}$ – $30^\circ\text{S}$ ) zonal mean quantities for each simulation. The quantities are  $q$ , the general circulation model's water vapor concentration at 70 hPa;  $q_{CC}$ , an estimate of water vapor entering the stratosphere based solely on the Clausius-Clapeyron relation over the  $10^\circ\text{N}$ – $10^\circ\text{S}$  region (see text for details);  $q_{LDP}$ , Lagrangian Dry Point estimate of  $q$  at 75 hPa ( $\sim 18.2$  km); and  $q_{LDP+ice}$  an estimate from a modified Lagrangian Dry Point method, where encountered ice is sublimated until the saturation limit is reached (as described in Section 2.2). Error bars denote standard deviation in deseasonalised monthly mean timeseries. The coefficients of determination ( $R^2$ ) (numbers superimposed on bars) are from the deseasonalised monthly mean timeseries relative to  $q$  of the same simulation, except that the correlations for  $q_{CC}$  are calculated with a lag of 1 month to account for upwelling time for air parcels from the dry point tropopause to 70 hPa. (b) For the quantities displayed in (a), the change for each of  $2 \times \text{CO}_2$  and  $4 \times \text{CO}_2$  expressed as a factor increase with respect to CONTROL.

#### 4. Lagrangian Analysis of Changes in Stratospheric Water Vapor

Whilst the grid-point based diagnostics presented in the previous section suggest that changes in convective injection contribute to the modeled increases in stratospheric water vapor as  $\text{CO}_2$  concentration is increased, the quantitative contribution remains unclear. For example, whilst increases in sublimation are shown in Figure 2e, some of this sublimation may correspond to ice that has formed in-situ in the TTL (as evidenced by the green line in Figure 1d) rather than being injected by convection (i.e., the light blue lines in Figures 1a and 1c). Therefore to examine further the impact of convective processes on stratospheric water vapor this section uses LDP calculations to complement the grid-point based diagnostics.

The entry amount of water vapor is estimated by the tropical mean concentration of water vapor at 70 hPa (18.6 km), which is above the minimum in the mean water vapor profile in all three simulations considered here. The entry amount of water vapor increases by a factor of 1.5 and 2.3 in the  $2 \times \text{CO}_2$  and  $4 \times \text{CO}_2$  simulations, respectively (Figure 3b, blue bars).

Based on the Clausius-Clapeyron relation, a crude measure of how water vapor is affected by changes in large-scale temperatures across the simulations is the average saturation mixing ratio at local dry points (e.g., Figure 6 of Hardiman et al., 2015), shown in Figure 3 as  $q_{CC}$ . The spatial average of  $q_{CC}$  is taken over the  $10^\circ\text{N}$ – $10^\circ\text{S}$  region because this is where most of the lowest saturation mixing ratios are experienced (averaging over a broader latitude belt results in higher estimates of  $q_{CC}$  and lower correlation with  $q$ ). As explained, for example, by Smith et al. (2021),  $q_{CC}$  is expected to overestimate concentrations because it does not take account of the sampling of the lowest temperatures by air parcels as they move through the TTL and into the stratosphere. Also included in Figure 3a is the coefficient of determination ( $R^2$ ) between the deseasonalised monthly mean time series over 10 years generated by each measure and the corresponding time series of  $q$ . For  $q_{CC}$  in the CONTROL simulation, the  $R^2$  is 0.17, that is, the correlation is weak.

The standard Lagrangian estimate of water vapor concentration,  $q_{LDP}$ , underestimates  $q$  in all simulations, with larger underestimation as the  $\text{CO}_2$  value is increased, from 2 ppmv in CONTROL to 3.2 ppmv in  $2 \times \text{CO}_2$  and 4.5 ppmv in  $4 \times \text{CO}_2$ . This is to be expected because Lagrangian calculations are not affected by numerical diffusion and additional parameterized processes that are present in the climate model (e.g., Smith et al., 2021; Stenke et al., 2008). Proportionally, the underestimation of  $q$  by  $q_{LDP}$  is very similar in all three simulations at around 40%.

Taking the modified Lagrangian estimate  $q_{LDP+ice}$  described in Section 2.2 as an indicator of the effect of including convective hydration, it is found that the difference between  $q$  and  $q_{LDP+ice}$  is 21%–35% of the difference between  $q$  and  $q_{LDP}$ , so the underestimate has been significantly reduced. The estimated contribution of convective hydration is substantial, 26%–32% of the magnitude of  $q$ . The correlation coefficients for  $q_{LDP}$  are all greater than 0.6 and slightly less than those for  $q_{LDP+ice}$ . This suggests that adding the effect of convective hydration to the Lagrangian estimate increases the skill in reproducing the climate model results, with respect to interannual variability. The difference between  $q_{LDP+ice}$  and  $q_{LDP}$  is a measure of convective hydration and is seen to increase through the sequence of three simulations, as  $CO_2$  and SST increase. By this absolute measure convective hydration becomes more important as  $CO_2$  and SST increase.

An alternative measure of the role of different processes in determining the change in stratospheric water vapor entry at higher  $CO_2$  concentration is the proportional change relative to the CONTROL simulation. These proportional changes are shown in Figure 3b for each of the four quantities shown in Figure 3a. This shows the proportional changes are similar across all four quantities. Therefore, on the basis of this measure, the underestimate of water vapor concentrations by the LDP calculation ( $q - q_{LDP}$ ) and the estimate of the convective contribution ( $q_{LDP+ice} - q_{LDP}$ ), is similar in the  $2 \times CO_2$  and  $4 \times CO_2$  simulations.

As noted in the introduction, the estimate  $q_{LDP+ice}$  has some arbitrariness and the detail of the implementation is different between D2016 and here, with neither being defensible as ‘correct’. Other possible approaches to a modified LDP calculation, taking some account of convective hydration, are considered in the Supporting Information S1. The alternative LDP calculations reach the same conclusions as for the estimate  $q_{LDP+ice}$  discussed here.

## 5. Conclusions

This study has investigated the detailed water budget of a global climate model to quantify the potential influence of deep convection on stratospheric water vapor increase in  $CO_2$  perturbed climate states. Lagrangian calculations based on fields extracted from the climate model, which provide an estimate of water vapor based on LDPs, have been used to provide additional insight. Whilst it would be desirable to extend this across several models, the detailed diagnostics and high temporal resolution output required for the study are not standard output for model intercomparison projects. Subject to that cautionary note, some clear and useful conclusions have been obtained from this study.

It has been shown that the parameterized convective transport plays an important role in the total water budget in the TTL and makes a dominant contribution to maintaining the concentrations of ice at altitudes extending to 1 km or so above the dry point tropopause. As altitude increases the small difference between convective supply and sedimentation changes from being negative, implying loss of water vapor through freeze-drying, to positive, implying convective hydration, with the transition occurring 0.5–1 km above the average dry point tropopause. The frequency of convective penetration (indicated by convective supply of ice) reduces with altitude above the dry point tropopause. As the vertical scale for this transition corresponds to just three or four model levels, it is likely that there will be sensitivities to vertical resolution and to the precise location of model levels.

As has been found in previous studies, in response to increased atmospheric  $CO_2$  the dry point tropopause moves upwards and the temperature and hence saturation mixing ratio of water vapor at the tropical tropopause increases. Convection then reaches a higher altitude, but does not penetrate any further into the stratosphere above the local dry point tropopause and the relative distribution of convective injection events above this level remains unchanged. However, there is an increase in the overall number of convective injection events and sublimation events which may be interpreted as more frequent convective injection and, potentially, a larger contribution to the lower stratospheric water vapor budget.

Consistent with previous studies, the absence from the LDP calculation of processes that are present in the model leads to an underestimation of the modeled tropical lower stratospheric entry values. This underprediction is larger with increased  $CO_2$  concentrations, from 2 ppmv in CONTROL to 3.2 to 4.5 ppmv in  $2 \times CO_2$  and  $4 \times CO_2$ , respectively (comparing blue and green bars in Figure 3a). Modified LDP calculations that attempt to include convective hydration based on the model ice fields reduce the underprediction by 65%–80%. The difference between  $q_{LDP+ice}$  and  $q_{LDP}$  increases as  $CO_2$  increases (comparing red and green bars in Figure 3a), from 1.6 to 2.3

to 3 ppmv in CONTROL,  $2 \times \text{CO}_2$  and  $4 \times \text{CO}_2$ , respectively (D2016 Table 1 reports that convective ice injection increases their 21st century average  $\text{H}_2\text{O}_{\text{entry}}$  by 1.4–2.5 ppmv, depending on the model simulation and trajectory calculation). But, the ratio  $(q_{\text{LDP+ice}} - q_{\text{LDP}})/q$ , measuring the relative contribution from convective hydration, is roughly constant, remaining in the range 0.26–0.32 (Figures 3a and 3b). It needs to be remembered that convective hydration is in part controlled by the temperatures in the TTL, because it is determined by saturation mixing ratios at the altitudes to which convection penetrates, which depend both on the penetration altitude and the large-scale temperature field.

Our conclusion, that—as  $\text{CO}_2$  increases—the relative importance of convective injection in determining stratospheric water vapor concentrations remains roughly constant, is somewhat different from that of D2016. This point was difficult to see in D2016 because their results did not make it clear that there was a significant contribution from convective hydration in the climate of their present day reference period. The overall implications of our study are that convective hydration depends not only on the frequency and altitude of convective penetration into the stratosphere, but also on large-scale temperatures in the TTL, which determine saturation mixing ratios and hence how much convective ice can be converted into vapor. If, for a given change in  $\text{CO}_2$ , there was a very large increase in typical penetration altitudes, and hence in the corresponding saturation mixing ratio, relative to typical large-scale dry point altitude, the proportional effect of convective hydration would increase. For the particular climate model considered here, it seems that the change in convective hydration is approximately in proportion to the change in dry point saturation mixing ratios, so the proportional effect remains the same. In other words, changes in convection do not allow entry values of water vapor concentration to escape the constraint of the large-scale temperature fields.

### Conflict of Interest

The authors declare no conflicts of interest relevant to this study.

### Data Availability Statement

The key data and scripts to generate the contained figures are available from Smith et al. (2022).

### Acknowledgments

We are grateful for constructive discussions with Felix Ploeger, John Pyle and Paul Earnshaw. The OFFLINE program prepared by Stephan Fueglistaler and Sue Liu was a valuable resource for this research. J. W. Smith was funded by a Natural Environment Research Council (NERC) Industrial CASE PhD studentship with the Met Office (NE/M009920/1). P. H. Haynes acknowledges support from the IDEX Chaires d'Attractivité programme of l'Université Fédérale de Toulouse, Midi-Pyrénées. A. C. Maycock was supported by the European Union's Horizon 2020 research and innovation programme under grant agreement No 820829 (CONSTRAIN project), by a NERC Independent Research Fellowship (NE/M018199/1) and The Leverhulme Trust (PLP-2018-278). N. Butchart was supported by the Met Office Hadley Centre Programme funded by BEIS and Defra. This work used JASMIN, the UK collaborative data analysis facility.

### References

- Banerjee, A., Chiodo, G., Previdi, M., Ponater, M., Conley, A. J., & Polvani, L. M. (2019). Stratospheric water vapor: An important climate feedback. *Climate Dynamics*, 53(3–4), 1697–1710. <https://doi.org/10.1007/s00382-019-04721-4>
- Bushell, A. C., Anstey, J. A., Butchart, N., Kawatani, Y., Osprey, S. M., Richter, J. H., et al. (2020). Evaluation of the Quasi-Biennial Oscillation in global climate models for the SPARC QBO-initiative. *Quarterly Journal of the Royal Meteorological Society*, 1–31. <https://doi.org/10.1002/qj.3765>
- Butchart, N., Anstey, J. A., Hamilton, K., Osprey, S., McLandress, C., Bushell, A. C., et al. (2018). Overview of experiment design and comparison of models participating in phase 1 of the SPARC Quasi-Biennial Oscillation initiative (QBOi). *Geoscientific Model Development*, 11(3), 1009–1032. <https://doi.org/10.5194/gmd-11-1009-2018>
- Dauhut, T., Chaboureaud, J. P., Haynes, P. H., & Lane, T. P. (2018). The mechanisms leading to a stratospheric hydration by overshooting convection. *Journal of the Atmospheric Sciences*, 75(12), 4383–4398. <https://doi.org/10.1175/JAS-D-18-0176.1>
- Dessler, A., Ye, H., Wang, T., Schoeberl, M., Oman, L., Douglass, A., et al. (2016). Transport of ice into the stratosphere and the humidification of the stratosphere over the 21st century. *Geophysical Research Letters*, 43(5), 2323–2329. <https://doi.org/10.1002/2016GL067991>
- Eyring, V., Bony, S., Meehl, G. A., Senior, C. A., Stevens, B., Stouffer, R. J., & Taylor, K. E. (2016). Overview of the Coupled Model Inter-comparison Project Phase 6 (CMIP6) experimental design and organization. *Geoscientific Model Development*, 9(5), 1937–1958. <https://doi.org/10.5194/gmd-9-1937-2016>
- Forster, P. M. d. F., & Shine, K. P. (2002). Assessing the climate impact of trends in stratospheric water vapor. *Geophysical Research Letters*, 29(6), 101–104. <https://doi.org/10.1029/2001GL013909>
- Fueglistaler, S., Dessler, A. E., Dunkerton, T. J., Folkins, I., Fu, Q., & Mote, P. W. (2009). Tropical tropopause layer. *Reviews of Geophysics*, 47(1), RG1004. <https://doi.org/10.1029/2008RG000267>
- Hardiman, S. C., Boutle, I. A., Bushell, A. C., Butchart, N., Cullen, M. J. P., Field, P. R., et al. (2015). Processes controlling tropical tropopause temperature and stratospheric water vapor in climate models. *Journal of Climate*, 28(16), 6516–6535. <https://doi.org/10.1175/JCLI-D-15-0075.1>
- Keeble, J., Hassler, B., Banerjee, A., Checa-Garcia, R., Chiodo, G., Davis, S., et al. (2021). Evaluating stratospheric ozone and water vapour changes in CMIP6 models from 1850 to 2100. *Atmospheric Chemistry and Physics*, 21(6), 5015–5061. <https://doi.org/10.5194/acp-21-5015-2021>
- Khaykin, S., Pommereau, J.-P., Korshunov, L., Yushkov, V., Nielsen, J., Larsen, N., et al. (2009). Hydration of the lower stratosphere by ice crystal geysers over land convective systems. *Atmospheric Chemistry and Physics*, 9(6), 2275–2287. <https://doi.org/10.5194/acp-9-2275-2009>
- Khaykin, S. M., Moyer, E., Krämer, M., Clouser, B., Bucci, S., Legras, B., et al. (2022). Persistence of moist plumes from overshooting convection in the Asian monsoon anticyclone. *Atmospheric Chemistry and Physics*, 22, 3169–3189. <https://doi.org/10.5194/acp-22-3169-2022>
- Kim, J., Grise, K. M., & Son, S.-W. (2013). Thermal characteristics of the cold-point tropopause region in CMIP5 models. *Journal of Geophysical Research: Atmospheres*, 118(16), 8827–8841. <https://doi.org/10.1002/jgrd.50649>

- Kirk-Davidoff, D. B., Hints, E. J., Anderson, J. G., & Keith, D. W. (1999). The effect of climate change on ozone depletion through changes in stratospheric water vapour. *Nature*, *402*(6760), 399–401. <https://doi.org/10.1038/46521>
- Lee, K.-O., Dauhut, T., Chaboureau, J.-P., Khaykin, S., Krämer, M., & Rolf, C. (2019). Convective hydration in the tropical tropopause layer during the StratoClim aircraft campaign: Pathway of an observed hydration patch. *Atmospheric Chemistry and Physics*, *19*(18), 11803–11820. <https://doi.org/10.5194/acp-19-11803-2019>
- Lin, P., Paynter, D., Ming, Y., & Ramaswamy, V. (2017). Changes of the tropical tropopause layer under global warming. *Journal of Climate*, *30*(4), 1245–1258. <https://doi.org/10.1175/JCLI-D-16-0457.1>
- Liu, Y. S., Fueglistaler, S., & Haynes, P. H. (2010). Advection-condensation paradigm for stratospheric water vapor. *Journal of Geophysical Research*, *115*(D24), 1–18. <https://doi.org/10.1029/2010JD014352>
- Manabe, S., & Wetherald, R. T. (1967). Thermal equilibrium of the atmosphere with a given distribution of relative humidity. *Journal of the Atmospheric Sciences*, *24*(3), 241–259. [https://doi.org/10.1175/1520-0469\(1967\)024<0241:teotaw>2.0.co;2](https://doi.org/10.1175/1520-0469(1967)024<0241:teotaw>2.0.co;2)
- Maycock, A. C., Joshi, M. M., Shine, K. P., Davis, S. M., & Rosenlof, K. H. (2014). The potential impact of changes in lower stratospheric water vapour on stratospheric temperatures over the past 30 years. *Quarterly Journal of the Royal Meteorological Society*, *140*(684), 2176–2185. <https://doi.org/10.1002/qj.2287>
- Maycock, A. C., Joshi, M. M., Shine, K. P., & Scaife, A. a. (2013). The circulation response to idealized changes in stratospheric water vapor. *Journal of Climate*, *26*(2), 545–561. <https://doi.org/10.1175/JCLI-D-12-00155.1>
- Maycock, A. C., Shine, K. P., & Joshi, M. M. (2011). The temperature response to stratospheric water vapour changes. *Quarterly Journal of the Royal Meteorological Society*, *137*(657), 1070–1082. <https://doi.org/10.1002/qj.822>
- Methven, J. (1997). *Offline trajectories: Calculation and accuracy* (Vol. 44). Tech. Rep. University of Reading. Retrieved from <http://www.met.reading.ac.uk/~swrmethn/offline/>
- Oinas, V., Lacis, A. A., Rind, D., Shindell, D. T., & Hansen, J. E. (2001). Radiative cooling by stratospheric water vapor: Big differences in GCM results. *Geophysical Research Letters*, *28*(14), 2791–2794. <https://doi.org/10.1029/2001GL013137>
- Richter, J. H., Butchart, N., Kawatani, Y., Bushell, A. C., Holt, L., Serva, F., & Yukimoto, S. (2020). Response of the quasi-biennial oscillation to a warming climate in global climate models. *Quarterly Journal of the Royal Meteorological Society*, 1–29. <https://doi.org/10.1002/qj.3749>
- Romps, D. M. (2011). Response of tropical precipitation to global warming. *Journal of the Atmospheric Sciences*, *68*(1), 123–138. <https://doi.org/10.1175/2010JAS3542.1>
- Schoeberl, M. R., Jensen, E. J., Pfister, L., Ueyama, R., Avery, M., & Dessler, A. E. (2018). Convective hydration of the upper troposphere and lower stratosphere. *Journal of Geophysical Research: Atmospheres*, *123*(9), 4583–4593. <https://doi.org/10.1029/2018JD028286>
- Schwartz, M. J., Read, W. G., Santee, M. L., Livesey, N. J., Froidevaux, L., Lambert, A., & Manney, G. L. (2013). Convectively injected water vapor in the North American summer lowermost stratosphere. *Geophysical Research Letters*, *40*(10), 2316–2321. <https://doi.org/10.1002/grl.50421>
- Smith, J. W. (2020). *Timescales of processes controlling stratospheric water vapour entry to the stratosphere*. Doctoral dissertation. University of Cambridge. <https://doi.org/10.17863/CAM.50382>
- Smith, J. W., Bushell, A. C., Haynes, P. H., Butchart, N., & Maycock, A. C. (2022). *Water budget and Lagrangian analysis of tropical tropopause in simulations with Hadley Centre Global Environmental Model version 3 (HadGEM3)*. NERC EDS Centre for Environmental Data Analysis. <https://doi.org/10.5285/e4eac61c06e348389f16bb863334dbf6>
- Smith, J. W., Haynes, P. H., Maycock, A. C., Butchart, N., & Bushell, A. C. (2021). Sensitivity of stratospheric water vapour to variability in tropical tropopause temperatures and large-scale transport. *Atmospheric Chemistry and Physics*, *21*(4), 2469–2489. <https://doi.org/10.5194/acp-21-2469-2021>
- Solomon, S., Rosenlof, K. H., Portmann, R. W., Daniel, J. S., Davis, S. M., Sanford, T. J., & Plattner, G.-K. (2010). Contributions of stratospheric water vapor to decadal changes in the rate of global warming. *Science*, *327*(5970), 1219–1223. <https://doi.org/10.1126/science.1182488>
- Stenke, A., & Grewe, V. (2005). Simulation of stratospheric water vapor trends: Impact on stratospheric ozone chemistry. *Atmospheric Chemistry and Physics*, *5*(5), 1257–1272. <https://doi.org/10.5194/acp-5-1257-2005>
- Stenke, A., Grewe, V., & Ponater, M. (2008). Lagrangian transport of water vapor and cloud water in the ECHAM4 GCM and its impact on the cold bias. *Climate Dynamics*, *31*(5), 491–506. <https://doi.org/10.1007/s00382-007-0347-5>
- Wagner, W., Riethmann, T., Feistel, R., & Harvey, A. H. (2011). New equations for the sublimation pressure and melting pressure of H<sub>2</sub>O ice Ih. *Journal of Physical and Chemical Reference Data*, *40*(4), 043103. <https://doi.org/10.1063/1.3657937>
- Walters, D., Baran, A. J., Boutle, I., Brooks, M., Earnshaw, P., Edwards, J., et al. (2019). The Met Office Unified Model Global Atmosphere 7.0/7.1 and JULES Global Land 7.0 configurations. *Geoscientific Model Development*, *12*(5), 1909–1963. <https://doi.org/10.5194/gmd-12-1909-2019>
- Werner, F., Schwartz, M. J., Livesey, N. J., Read, W. G., & Santee, M. L. (2020). Extreme outliers in lower stratospheric water vapor over North America observed by MLS: Relation to overshooting convection diagnosed from colocated Aqua-MODIS data. *Geophysical Research Letters*, *47*(24), e2020GL090131. <https://doi.org/10.1029/2020GL090131>
- Wright, J. S., Fu, R., Fueglistaler, S., Liu, Y. S., & Zhang, Y. (2011). The influence of summertime convection over Southeast Asia on water vapor in the tropical stratosphere. *Journal of Geophysical Research*, *116*(D12), D12302. <https://doi.org/10.1029/2010JD015416>